Depth compression based on mis-scaling of binocular disparity may contribute to angular expansion in perceived optical slant

Zhi Li

Psychology Department, Swarthmore College, Swarthmore, PA, USA

Frank H. Durgin

Psychology Department, Swarthmore College, Swarthmore, PA, USA

Three studies, involving a total of 145 observers examined quantitative theories of the overestimation of perceived optical slant. The first two studies investigated the depth/width anisotropies on positive and negative slant in both pitch and yaw at 2 and 8 m using calibrated immersive virtual environments. Observers made judgments of the relative lengths of extents that were frontal with those that were in depth. The physical aspect ratio that was perceived as 1:1 was determined for each slant. The observed anisotropies can be modeled by assuming overestimation in perceived slant. Three one-parameter slant perception models (angular expansion, affine depth compression caused by mis-scaling of binocular disparity, and intrinsic bias) were compared. The angular expansion and the affine depth compression models provided significantly better fits to the aspect ratio data than the intrinsic bias model did. The affine model required depth compression at the 2 m distance; however, that was much more than the depth compression measured directly in the third study using the same apparatus. The present results suggest that depth compression based on mis-scaling of binocular disparity may contribute to slant overestimation, especially as viewing distance increases, but also suggest that a functional rather than mechanistic account may be more appropriate for explaining biases in perceived slant in near space.

Introduction

The perception of locomotor space includes a number of striking geometrical errors. For example, egocentric distance is underestimated by as much as 0.7 (e.g., Foley, Ribeiro-Filho, & Da Silva, 2004; Kelly, Loomis, & Beall, 2004); hill slant (both uphill and downhill) is overestimated by as much as 20° (Kammann, 1967; Proffitt, Bhalla, Gossweiler, & Midgett, 1995); exocentric extents in depth are increasingly compressed as viewing distance becomes larger (e.g., Gilinsky, 1951); and in-depth extent is foreshortened relative to frontal extent in both horizontal and vertical dimensions (e.g., Foley et al., 2004; Higashiyama, 1996; Loomis, Da Silva, Fujita, & Fukusima, 1992; Wagner, 1985). An angular scale expansion theory has been developed in the past few years that has the goal of explaining many of these empirical spatial biases. For example, the angular expansion theory has provided quantitative explanations of empirical observations of linear compression of perceived egocentric distance (Durgin & Li, 2011), nonlinear compression of perceived exocentric distance (Li & Durgin, 2012), foreshortening of in-depth extent relative to both vertically and horizontally frontal extents (Li, Phillips, & Durgin, 2011; Li et al., 2013), and overestimation of both uphill and downhill slopes (Li & Durgin, 2009, 2010).

The angular scale expansion theory has two fundamental assumptions: First, two angular variables (optical slant and gaze/angular declination) are perceptually expanded in their most relevant range to the locomotion space. Second, once this angular expansion is accounted for, Euclidean geometry can be applied to the perceived spatial variables within local visual space. To account for a wide range of empirical observations, the angular expansion theory employs two quantitative models: one for optical slant and the other for gaze/angular declination (see Li & Durgin, 2012, for a short review). Both models were developed from independent sets of empirical observations. For example, the slant model was first proposed based on slant estimation data with both explicit and implicit measures (Li & Durgin, 2010), and was later simplified as Equation 1 (Li & Durgin, 2012). The model describes the

Citation: Li, Z., & Durgin, F. H. (2013). Depth compression based on mis-scaling of binocular disparity may contribute to angular expansion in perceived optical slant. *Journal of Vision*, *13*(12):3, 1–18, http://www.journalofvision.org/content/13/12/3, doi:10.1167/13.12.3.

doi: 10.1167/13.12.3 Received March 14, 2013; published October 4, 2013 ISSN 1534-7362

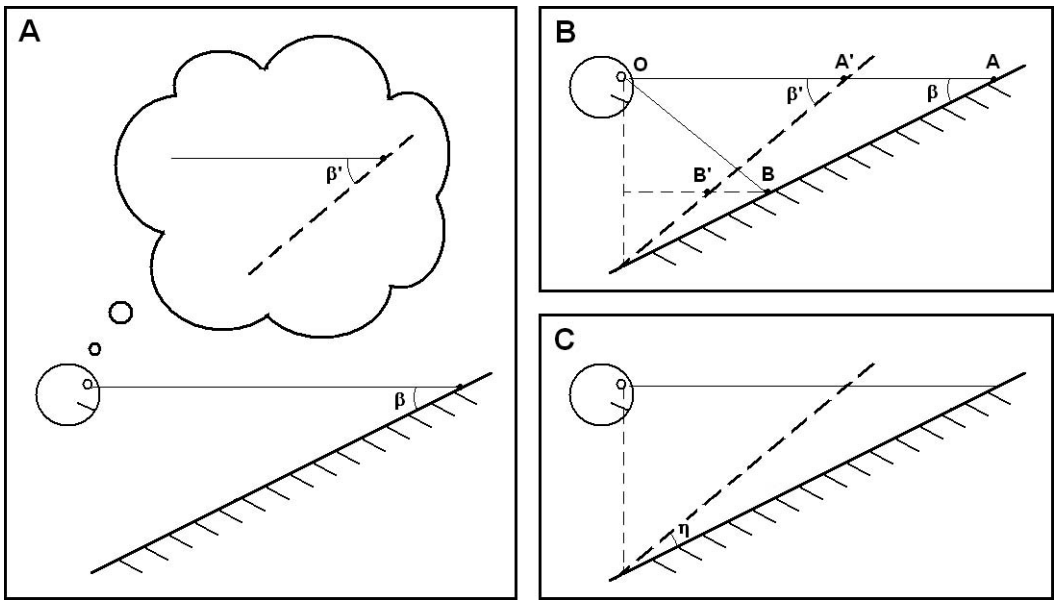

Figure 1. Angular scale expansion in perceived slant and two possible sources for this angular expansion. According to the angular expansion hypothesis, perceived slant is exaggerated (A). There are at least two possible sources for the angular expansion: affine depth compression along the line of sight caused by mis-scaling of binocular disparity (B), and overestimation of geographical slant caused by intrinsic bias of perceived ground plane (C).

observation by Li and Durgin (2010) that perceived slant, in the range of 6°–36° from horizontal, is nearly a linear function of actual slant (with a gain of 1.5) while the intercept of the slant function increases proportionally to the log of viewing distance. Bridgeman and Hoover (2008) have also reported increases in perceived slant as a logarithmic function of viewing distance.

$$\beta' = 1.5\beta + k \ln(D), \quad (1)$$

where β' is perceived slant, β is actual slant, D is viewing distance, and k is a constant.

Equation 1 provides an excellent fit to existing verbal hill slant estimation data (e.g., Proffitt et al., 1995, see the model prediction in Li & Durgin, 2010), as well as to exocentric in-depth extent perception data (e.g., Gilinsky, 1951, see the model prediction in Li & Durgin, 2012), as well as the distance anisotropy data observed in aspect ratio tasks (e.g., Kudoh, 2005; Loomis & Philbeck, 1999, see the model prediction in Li & Durgin, 2010). At present, however, it is not a complete model of perceived optical slant because it does not predict slant saturation at 90° optical slant. That is, an optical slant perpendicular to the line of sight should be perceived as approximately 90° optical slant. The reason that Equation 1 can nonetheless fit so much empirical data is because it is developed from slant estimation data with shallow slants (i.e., 6° to 36°—hills are rarely steeper than this) and the relevant empirical data concerning perceived extents in depth along the ground also reflect shallow optical slants.

One purpose of the present study is to extend the optical slant model to resolve the 90° saturation issue. Hibbard, Goutcher, O'Kane, and Scarfe (2012) have recently reported data relevant to the more frontal case using disparity cues alone in an aspect ratio task involving slanted surfaces.

Equation 1 is essentially a mathematically descriptive model. It suggests that perceived optical slant is overestimated (Figure 1A) but it does not indicate what may cause the angular expansion. Several alternative kinds of theory have previously been adduced to account for biases in space perception. Some also predict slant overestimation. Because some of those theories have assumed detailed mechanisms that may cause perceptual biases, we will evaluate, in the present study, which of the proposed mechanisms is more likely to contribute to the slant biases we have observed. This could reinforce the angular scale expansion theory by testing possible source of angular expansion in the perception of slant. We will focus on two candidate theories: the hypothesis of depth compression (e.g., Ross, 1974; especially *affine* depth compression, Wagner, 1985), and the intrinsic bias hypothesis (Ooi, Wu, & He, 2006).

Perhaps the most popular explanation of the many biases observed in space perception is the hypothesis of a non-Euclidean visual space (e.g., Battro, Netto, & Rozestraten, 1976; Blank, 1953; Doumen, Kappers, & Koenderink, 2005; Foley, 1964; Foley et al., 2004; Indow, 1991; Levin & Haber, 1993; Kelly et al., 2004; Koenderink, vanDoorn, & Lappin, 2000; Luneburg

1947, 1950; Norman, Crabtree, Clayton, & Norman, 2005; Todd, Oomes, Koenderink, & Kappers, 2001; Wagner, 1985; see also Wagner, 2006 for an extensive review). The prominent foreshortening of in-depth extent relative to frontal extent is often thought of as evidence that the visual space may approximate an affine geometry, in which the depth along any sagittal horizontal axis is compressed whereas the depth along any frontal parallel axis remains uncompressed. Under such an assumption, slant will be exaggerated (Figure 1B). As Wagner (1985) pointed out, it seems unlikely that the depth compression is actually along a fixed axis in a fixed Cartesian coordinate system. It would be quite reasonable to assume depth compression occurs along the line of sight because human visual experience can be best described in terms of a polar coordinate system. Although the models proposed by Wagner (i.e., the affine contraction model and the vector contraction model) were also pure mathematically descriptive models, it turns out that the idea of affine compression along line of sight (Wagner's vector contraction model) is roughly consistent with the mis-scaling of binocular disparity information. That is, if viewing distance to the fixation point is foreshortened, the disparity map formed by the difference between the two retinal images would rescale the implied distance to every point on a slanted surface, which in turn would result in overestimation of the slant. In fact, in the limit (for a small field of view), the effect of slant exaggeration under the assumption of mis-scaling of binocular disparity is functionally equivalent to that under the assumption of affine depth compression along line of sight (see Appendix A). Thus, the mis-scaling of binocular disparity seems to be a plausible mechanism for angular expansion of slant.

Another mechanism that might cause slant exaggeration is proposed in the intrinsic bias hypothesis, which assumes that the default (internal) representation of ground plane is tilted upward (Ooi, Wu, & He, 2006). This intrinsic bias would make the perceived geographical slant of a flat ground plane appear tilted upward and this constant slant error is additive to any ground surface that is slanted (Figure 1C) (Ooi & He, 2007).

In the present study, to extend the optical slant model (Equation 1), we first propose a new model attempting to explain perception of slant with a wider range of slants across different viewing distances. To test this new slant model, we collected implicit slant estimation data in Experiment 1, using an aspect ratio task. The slants ranged from 9° to 90° at two viewing distances. These data will be used to evaluate the performance of the new model. The performance of the other two models (i.e., the affine depth compression along line of sight and the intrinsic bias model) will also be evaluated and compared.

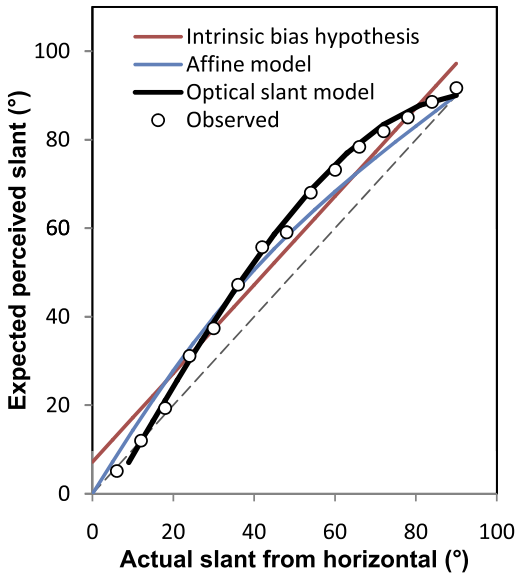

Figure 2. The best model fits to previously observed slant estimation data (open circles). The red line is the best fit for the intrinsic bias model, assuming a constant slant error of 7.2° (sum of squared errors, $SSE = 407.66$). The blue line is the best fit of the affine model based on mis-scaling of binocular disparity, assuming a distance compression ratio of 0.69 ($SSE = 248.61$). The black line is the best fit of Equation 3, assuming the viewing distance is 0.5 m and $k = 10.8$ ($SSE = 30.64$).

The new optical slant model

When surfaces within reachable distance are viewed with a horizontal gaze so that optical slant is equivalent to the geographical slant (surface orientation relative to horizontal), perceived geographical slant is exaggerated in the range of shallow slants but smoothly saturates toward vertical or 90°, as shown in Figure 2 (Durgin, Li, & Hajnal, 2010). This visual slant bias is highly consistent with orientation bias from haptic slant perception, and both these slant functions can be approximated by a scaled sine function (Equation 2) (Durgin & Li, 2012).

$$\beta' = 90^\circ \sin(\beta) \quad (2)$$

While Equations 1 and 2 are apparently two quite different models, they are actually very similar for shallow slants at short viewing distances. At a short viewing distance, $k \ln(D)$ becomes negligible (for example, when $D = 1$ m, $\ln(D) = 0$). For shallow slants, $\sin(\beta)$ approximates β (in radians), while 90° is 1.57 (in radians). Thus, both models would approximately degenerate to $\beta' = 1.5\ \beta$ for shallow slants at short viewing distance. It is possible to unify the two models by keeping the sine function in Equation 2 (for the sake of the 90° saturation) while also including the log-distance term in Equation 1 (to simulate the distance

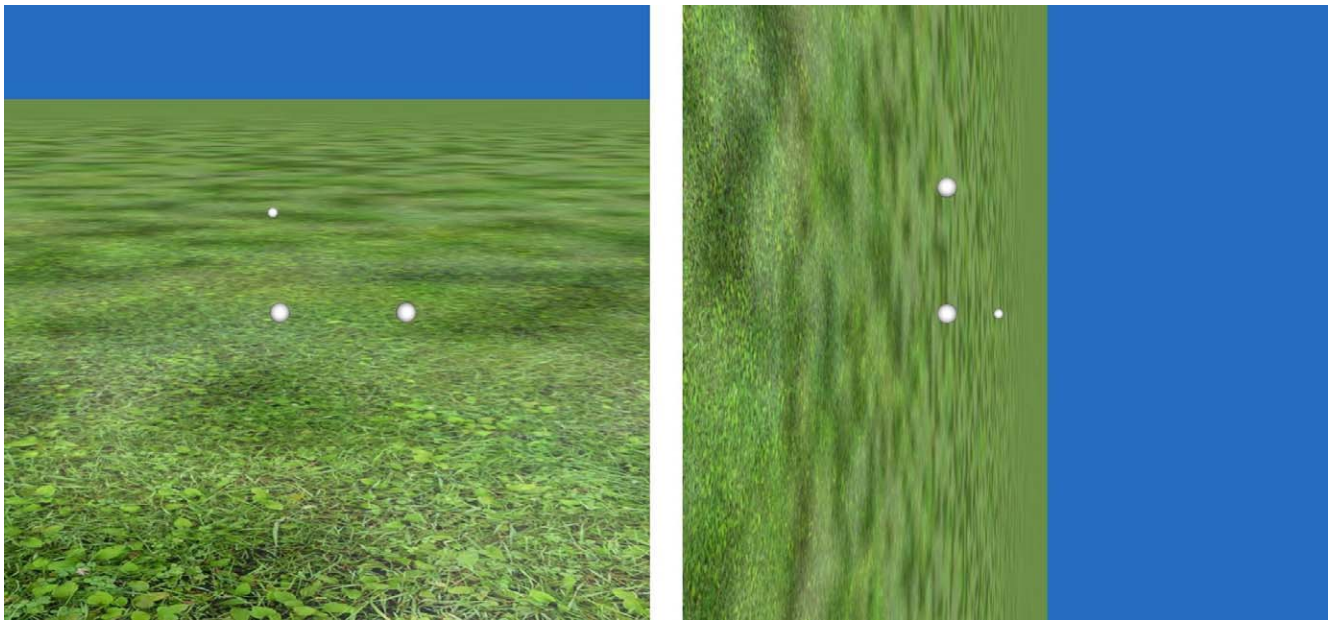

Figure 3. Sample images of the visual stimuli used in Experiment 1. Left, a pitch slant (an uphill surface). Right, a yaw slant (a rightward tilted surface). Surfaces were viewed in stereo in a calibrated immersive head mounted display.

effect). Equation 3 describes a candidate for such unified model. The cos(β) added to the log-distance term is to force the perceived optical slant β' to 90° when actual optical slant β is 90°. We will refer to Equation 3 as the new optical slant model.

$$\beta' = 90° \sin(\beta) + k \ln(D) \cos(\beta), \quad (3)$$

where β' is perceived slant, β is actual slant, D is viewing distance, and k is a constant.

Figure 2 shows that the new optical slant model provides a fairly good fit (thick black line) to the observed slant estimation data in reachable distance (averaged from visual and haptic slant estimation, Durgin & Li, 2012). And it is apparently better than the best fit of the intrinsic bias model (red line) and that of the affine depth compression model based on mis-scaling of binocular disparity (blue line) (see Appendix A for details).

Experiment 1

In order to evaluate the performance of the new optical slant model (i.e., Equation 3) in modeling slant estimation at farther viewing distances, we conducted Experiment 1. We sought to estimate the simulated aspect ratio required to make an L-shaped arrangement of balls on a tilted surface appear equilateral. We tested a large range of slants (9° to 90° with regard to the line of gaze) at two viewing distances (2 and 8 m). Our methods were similar to those used in Li and Durgin (2010), but with a few changes. Li and Durgin only tested uphill slants. In the present study, we sought to generalize their result and therefore examined slants in four directions—two directions in pitch (uphill and downhill) and two directions in yaw (leftward tilted and rightward tilted). If the slant bias is due to the intrinsic representation of the ground plane, as proposed by the intrinsic bias hypothesis, there should be substantial differences across the four slant directions. For example, the bias in perceived aspect ratio should be reversed for downhill slant as opposed to that for uphill slant. But if slant overestimation is purely a phenomenon of perceived optical slant, or if is due to affine depth compression along line of sight, there may not be any difference across the four slant directions.

Methods

Participants

Ninety-seven Swarthmore undergraduates (57 female, 40 male) participated in this experiment. All the participants had normal or corrected-to-normal vision. None of them had prior experience with the aspect ratio task. The experimental procedures reported here were approved by the local research ethics committee and were conducted in accordance with the Declaration of Helsinki.

Task

On each trial, participants viewed an arrangement of three balls forming an L shape on a slanted surface (Figure 3). They simply needed to indicate which leg of

the L appeared longer. Prior to participation, the task was explained to participants with the help of a diagram. Once it was clear that the participant understood the task, they were fitted with the head mounted display (HMD) and given a radio mouse to use for their responses. The 240 trials of the experiment took about 20 min to complete.

Apparatus

The aspect ratio stimuli were simulated in an immersive virtual environment presented in an nVisor SX HMD with a nominal resolution of 1280 × 1024 and 60-Hz refresh rate. Display images were pincushion corrected, using Vizard 4 (WorldViz Co.). An optical tracking system (VICON) was used to monitor the participant's head position and orientation. The head position and orientation was then used to update the display of the HMD with a lag of less than 100 ms. We used a fixed (60 mm) interpupillary distance (IPD) in this experiment, unlike the study of Li and Durgin (2010) who had measured IPD for each observer and used individual values in their simulations. The vertical field of view (FOV) subtended 34°. A simulated dark aperture restricted each eye's horizontal FOV to about 33° with about 80% binocular overlap, which reduced the discomfort caused by the physical frames of the HMD screens (Durgin & Li, 2010). Without this simulated aperture, the edges of the display (which have 100% binocular overlap) are binocularly specified to be infinitely far away; however the virtual aperture they form necessarily seems to occlude (i.e., form a window around) near surfaces in the virtual scene. To remove this anomalous occlusion of near surfaces by a far window, the simulated aperture replaces the edges of the display with a virtual window that is about 11 cm in front of the eyes so that occlusion of the edges of the scene by this aperture seems appropriate.

Slant displays

The visual stimuli were composed of a large tilted surface (2000 m × 2000 m) with grassy texture and three identical white spheres lying on the surface (Figure 3). A uniform blue background (sky) was used. The three spheres were always arranged in an L shape, with the sphere at the corner of the L being always simulated at eye level. Ten slant angles (9° to 90° by 9° intervals, specified with regard to the line of gaze at the corner sphere) at each of two viewing distances (2 and 8 m from the corner sphere) were tested for each surface direction.

Design

A between subject design was used so that the 97 participants were assigned to eight groups and each participant only saw one direction of surface slant at one viewing distance. Due to a scheduling error, 13 participants were assigned to the group with leftward tilted slant at 2 m. Each other group had 12 participants.

On each trial, the three white spheres (arranged in an L shape) were shown on the tilted surface. The participant's task was to compare the distance of the two legs of the L along the surface and decide which one was longer. The sphere at the corner of the L shape was at eye level, with a fixed visual angle of 1.14° for both viewing distances. The length of the frontal extent of the L-shape subtended a constant visual angle of about 7.15° and was scaled proportionally to viewing distance. The angular length of the in-depth extent of the L shape was determined by the physical aspect ratio (in-depth/frontal) that was between 0.33 and 8.14. A logarithmic up-down staircase procedure was used to simultaneously measure the PSEs (points of subject equality) between in-depth and frontal lengths for all 10 slants. There were 20 interleaved staircases. For each slant, one staircase started with a small physical aspect ratio (i.e., x^{-8}) and the other started with a big physical aspect ratio (i.e., x^{15}). The base x decreased with the slant (i.e., x was 1.15, 1.14, 1.13, 1.12, 1.11, 1.10, 1.09, 1.08, 1.07, and 1.06 for the 10 slants, respectively). The stimuli were shown in blocks. In each block, 1 of the 20 staircases was shown once in a random order. There were 12 blocks for each participant. On each trial, a two-alternative forced-choice (2AFC) response was collected by means of key presses to indicate whether the in-depth extent appeared longer or shorter than the frontal extent. The physical aspect ratio of the next trial in that staircase was adjusted up or down by a variable multiplicative step size (achieved by adding or subtracting from the exponent), depending on the response given and the block number in that staircase. Initial step size was by increasing or decreasing the exponent by eight; this step size declined to four after the first block and to two after the fourth block, where it remained thereafter.

Data analysis

The aspect ratio defined in the present study is always the ratio between the in-depth and the frontal extent. Whereas the retinal projection of the in-depth extent on the pitch slant is oriented vertically, the retinal projection of the in-depth extent on the yaw slant is oriented horizontally. If the vertical extent on the retinal image is exaggerated relative to the horizontal extent because of the horizontal-vertical illusion, the foreshortening of the in-depth extent on the pitch slant would be less than that on the yaw slant. So, the perceived aspect ratio matches on pitch slant would be less biased than that on the yaw slant. To

compensate for the HVI (horizontal-vertical illusion) effect, the aspect ratios of each participant at each amount of slant can be normalized (i.e., divided) by their own aspect ratio data in the 90° slant condition. Our planned analyses tested for this possibility.

Results

Points of subjective equality (i.e., PSE) were computed for each slant for each participant using a logistic psychometric function on log aspect ratio. A mixed-effects model of the complete data set including *axis of slant* (yaw or pitch), *direction of slant* (positive or negative), *amount of slant* (degrees), and *viewing distance* (meters), and all two-way interactions between these four factors revealed no interaction between axis of slant and the other factors, and no effects of direction of slant, but it did show that the slants in yaw produced larger aspect ratios than did slants in pitch, $t(943) = 2.049$, $p = 0.041$. Because this effect is consistent with a horizontal-vertical illusion (HVI), and Hibbard et al. (2012) have shown that the HVI is not caused by slant perception, we normalized each aspect ratio for each axis of slant by the matched aspect ratio (PSE) for each observer in the case of the frontal (90°) slants. When the same mixed-effects linear model was conducted on such normalized data, there was no longer any main effect of axis of slant, $t(943) = 0.67$, $p = 0.503$, nor were there any reliable interactions with axis of slant. Thus, the first observation to be made is that, once the horizontal-vertical illusion is taken into account, the implicitly estimated slant did not differ across the four directions we tested.

We therefore eliminated axis of slant from the model of normalized aspect ratios (as well as direction of slant, which had no effect in any of the models). The resulting mixed-effects model gave evidence of higher aspect ratios for lower slants, $t(959) = 4.54$, $p < 0.0001$; higher aspect ratios at farther distances, $t(959) = 4.32$, $p < 0.0001$; and it also indicated that the distance effect was more pronounced for lower slants, $t(959) = 4.02$, $p < 0.0001$. Figure 4 depicts the relationship between distance and perceived aspect ratio (with HVI correction) as a function of slant, collapsed across slant direction.

One interesting finding emerged during the HVI normalization process: Whereas the amount of HVI in the 90° pitch slant condition is 11%, the HVI in the 90° yaw slant condition was negligible (only −2%). An ANOVA confirmed that the HVI was reliably greater on frontal surfaces in the context of pitch slants than in the context of yaw slants, $F(1, 88) = 27.3$, $p < 0.0001$. (There was no difference between uphill and downhill slants.) This difference between the yaw and pitch conditions is interesting because the frontal stimuli in the two slant conditions were essentially the same, so that the absence of a prominent HVI effect in the 90° yaw slant is most likely related to the presence of yaw slants on other trials. An HVI magnitude of about 5%–6% is quite typical, and the difference between these two conditions corresponds to the sum of two 6% HVI effects. Hibbard et al. (2012) argued that the HVI is not due to a bias in perceived slant in depth. We thought it worth noting that the HVI measured on frontal surfaces in our study differed as a function of the possibility of surface tilt would be in yaw or in pitch. This may show that, independent of perceived slant, the visual system seeks to take into account likely slant when evaluating exocentric extents that might or might not be in depth.

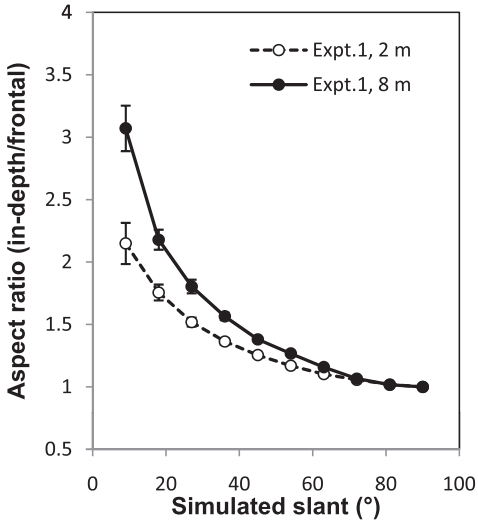

Figure 4. The results of Experiment 1: aspect ratios at the mean PSEs (with HVI correction) as a function of amount of slant and viewing distance. The data were collapsed across axis of slant and direction of slant. Standard errors are shown.

Another unexpected observation was that the aspect ratio data was systematically lower than those from the report of Li and Durgin (2010). We will take up this second issue in Experiment 2.

Model performance

The aspect ratio data measured in Experiment 1 can be used to quantitatively evaluate the performance of the three models we have considered (i.e., the new optical slant model, the affine model based on mis-scaling of binocular disparity, and the intrinsic bias model). A detailed derivation of the predictions of the three models is presented in Appendix A. Each of the three models is a one-parameter model. In brief, the parameter k, for the new optical slant model is a free parameter. The parameter c, for the affine model, refers to the amount (ratio) of depth compression along the

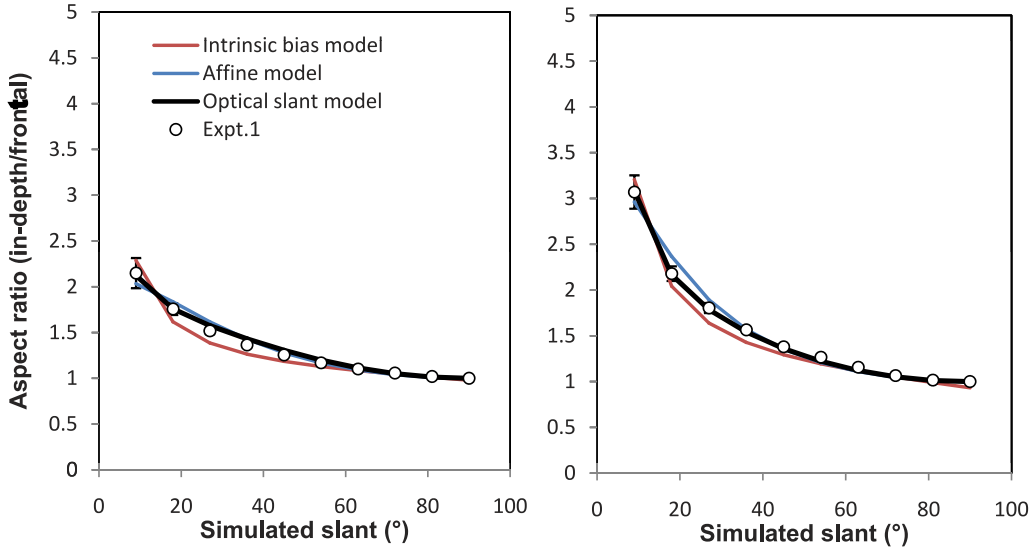

Figure 5. Observed aspect ratio data of Experiment 1 (open circles) and the best fits of the three theoretical models (intrinsic bias model—red lines, affine model—blue lines, and the new optical slant model—black lines) for the 2 m (left panel) and 8 m (right panel) distances, respectively. The parameter values and the sum of squared error (*SSE*) of the best model fit at the two distances are: $\eta = 11.968°$ ($SSE = 0.0741$), $c = 0.472$ ($SSE = 0.0340$), $k = 7.764$ ($SSE = 0.0121$) for the 2 m fit, and $\eta = 21.114°$ ($SSE = 0.1033$), $c = 0.303$ ($SSE = 0.0623$), $k = 7.191$ ($SSE = 0.0052$) for the 8 m fit.

line of sight at the fixation distance. The parameter η, for the intrinsic bias model, refers to the additive slant exaggeration error supposed by that model. The best fit for each of the three models is shown in Figure 5 along with the observed aspect ratio data. Note, the best-fitting model parameters were computed separately for the two viewing distances in all three models to make the fits comparable, although k is expected to be largely independent of viewing distance. The sum of squared error (SSE) was computed for each model fit at each viewing distance. The SSEs for the new optical slant model (0.012 at 2 m and 0.005 at 8 m) are the smallest among the three. The SSEs for the intrinsic bias model (0.074 at 2 m and 0.103 at 8 m) are the largest. The SSEs for the affine model (0.034 at 2 m and 0.062 at 8 m) are in the middle. Thus, the new optical slant model provided the best fit to the averaged aspect ratio data at both viewing distances.

To more formally compare the models we fit the aspect ratios (PSEs) of each individual participant with the three models separately. The SSEs for each individual fit were computed. A paired Student t test of the SSEs between each pair of the models at the two viewing distances revealed no significant difference between the new optical slant model and the affine model at both 2 m, $t(48) = 1.33$, $p = 0.19$, and 8 m, $t(47) = 0.52$, $p = 0.60$; but the SSEs of the intrinsic bias model were significantly greater than that of the new optical slant model at 2 m, $t(48) = 3.00$, $p < 0.01$, and 8 m, $t(47) = 4.63$, $p < 0.001$; and they were also significantly larger than that of the affine model at 2 m, $t(48) = 4.54$, $p < 0.001$, and at 8 m, $t(47) = 3.73$, $p < 0.001$ (Figure 6).

The individual estimates of c in the affine model were reliably smaller at 8 m ($M = 0.35$) than at 2 m ($M = 0.52$), $t(96) = 4.04$, $p = 0.00016$, consistent with greater depth compression at farther distance. In contrast, and as expected, for the new optical slant model there was no reliable difference between the individual estimates of k in the 2 m ($M = 8.2$) and the 8 m ($M = 7.8$) conditions, $t(96) = 0.13$, $p = 0.897$, suggesting that k in the new optical slant model is independent of viewing distance.

Discussion

One purpose of the present study was to test whether the new optical slant model can account for slant perception at different viewing distances and with a wider range of slant (up to 90°) than the original optical slant model (i.e., Equation 1). The results in Experiment 1 suggest that the new optical slant model is indeed a pretty good descriptive model that not only fits explicit slant estimation data within reachable distance (i.e., Figure 2) but also fits implicit slant estimation data at father distances (i.e., Figure 5). Moreover, the parameter k in the new optical slant model remains independent of viewing distance, which suggests that the intercept of the slant function increases linearly with log distance for shallow slants (i.e., when $\cos(\beta)$ is close to one), as proposed by Li and Durgin (2010).

The other purpose of the present study was to evaluate two plausible mechanisms that may contribute

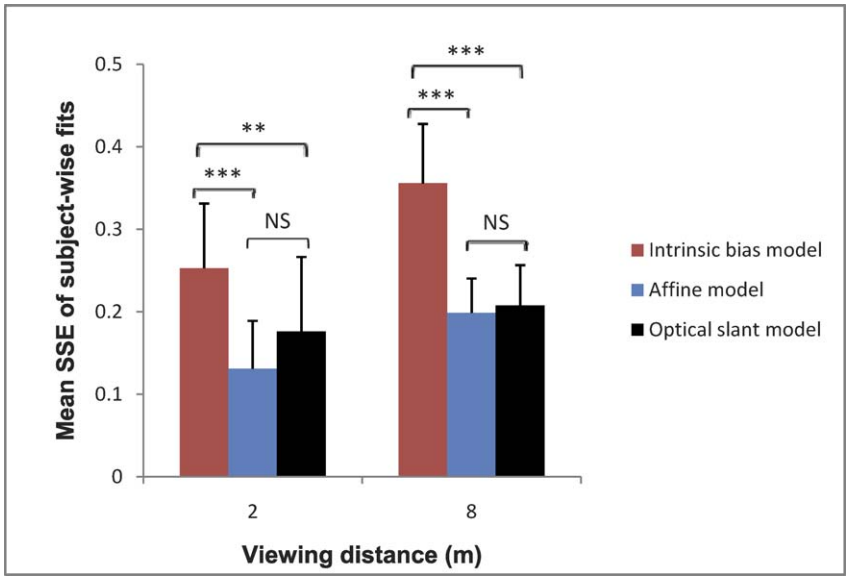

Figure 6. Mean *SSE*s of subject-wise fits of the three models to the aspect ratio data in Experiment 1. Results of paired *t* tests between each pair of the three models on the SSEs are shown. Standard error bars are shown.

to the angular expansion of perceived slant (i.e., affine-like depth compression due to mis-scaling of binocular disparity and the intrinsic bias of the perceived ground plane). Whereas Figure 5 suggested that both models can provide a reasonably good fit to the averaged aspect ratio data, the model fits to individual subjects' data indicated that the affine model fits were significantly better than the fits of the intrinsic bias model. Further evidence indicating that intrinsic bias is not a source of angular expansion in perceived optical slant is the fact that there was no significant difference in the perceived aspect ratios between the pitch and yaw slant conditions. Because the intrinsic bias is a bias of the perceived ground plane, it shouldn't have any effect on the perceived yaw slants. A related observation was reported by Bian and Andersen (2011) who showed that perceived aspect ratio on the ground is less biased than that on a ceiling when texture and motion parallex were the only information to specify the surfaces. If the intrinsic bias is the main cause of the bias in the perceived aspect ratio, the bias of the perceived aspect ratio on the ground plane should be larger than that on the ceiling whereas the findings of Bian and Andersen suggest that being a ground plane may actually serve as an addition cue to being actually horizontal. In the present study, we found no difference in the aspect ratio data between uphill and downhill slant, which is not contradictory to Bian and Andersen's finding, because there was no horizontal ground plane condition (which would be a special case) in our stimuli, whereas Bian and Andersen only examined horizontal planes.

In contrast to the prediction of the intrinsic bias model, the affine model based on mis-scaling of binocular disparity predicts no difference between pitch and yaw slants because it is the relative geometry between the observer and the slant that matters. Moreover, Li and Durgin (2010) concluded that the effect of viewing distance on perceived slant in their study (which provided an excellent model of real hill data) was purely due to binocular information because they scaled the texture size at different viewing distances so that texture was uninformative about distance. Thus, the mis-scaling of binocular disparity could very likely be a contributing source of angular expansion in perceived optical slant.

Whereas the mis-scaling of binocular disparity is a likely source of angular expansion in perceived optical slant (especially with increasing distance), it may not be the only source. Another important source that may affect perceived optical slant is texture information. We have mentioned in the results that the aspect ratios in the pitch slant condition were systematically lower than those reported in Li and Durgin (2010), in which only pitch slants were tested. There were two major differences between the two studies: the slant ranges tested were different and the monocular texture was scaled with viewing distance in one study but not in the other. In Experiment 2, we will examine which of the two factors may be the main cause that affected the aspect ratio data. If it turns out that monocular texture scaling is the primary cause, it will support the idea that texture information also plays a role in the angular expansion in perceived optical slant. Another reason to doubt that mis-scaling of binocular disparity provides a complete account for the slant bias comes from observed slant-estimation data. To best fit the explicit slant estimation data, the depth compression ratio, c, in

the affine model has to be set to 0.69 (Figure 2). This implies that in a full cue environment a viewing distance of 0.5 m (the rough viewing distance when collecting those explicit slant estimation data in Durgin et al., 2010) was underestimated. Underestimation of such a short distance is unlikely considering previous reports that binocular vision expands perceived depth in near space but compresses it in far space (e.g., Foley, 1985; Johnston, 1991; Philbeck & Loomis, 1997). The affine model fits to the present aspect ratio data suggest that depth compression ratios were about 0.5 at 2 m and 0.3 at 8 m in our virtual environment. In order to examine whether these affine-model-predicted depth compression ratios could be verified, in Experiment 3, we directly measured the depth compression ratio in our virtual environment.

Experiment 2

Because the judged aspect ratios in Experiment 1 were systematically lower than those reported by Li and Durgin (2010), we sought to investigate the cause of this discrepancy. There are many differences between the two studies. Minor differences were that the surface textures were different and there were some minor design differences. More major differences were that the tested slant ranges were different and that the size of the texture was scaled to viewing distance in one study but not in the other. That is, Li and Durgin scaled the texture so that it was the same retinal size across viewing distances, which were tested within-subjects; in Experiment 1 (a between-subject study), we let retinal texture size differ as a function of viewing distance). In Experiment 2, we reduced the range of slants to 6° to 24° (matched that in Li and Durgin) and manipulated texture scaling, so that we could see if either of these manipulations could explain the data differences between the two studies.

Methods

Twenty-eight undergraduates (12 female; 16 male) from Swarthmore College participated in this experiment. All the participants had normal or corrected-to-normal vision. None of them had participated in Experiment 1.

Visual stimuli were shown in the same virtual environment as that used in Experiment 1. The texture of the surface was identical to that used in Experiment 1. The range of slants was reduced so that only four slants (6°, 12°, 18°, and 24°) were tested. In addition, only one pitch slant (uphill) and one yaw slant (rightward) were tested. Two distances (2, 8 m) were used. Similar to Li and Durgin (2010), a within subject design was used so that each participant saw all the 16 (Direction of Slant × Viewing Distance × Amount of Slant) combinations. To investigate the effect of texture scaling, half the participants were presented with the size of the texture being rescaled to compensate for the different viewing distance (i.e., it maintained the same retinal size at different binocular distances, replicating Li & Durgin, 2010) while the other half were tested without this artificial scaling of texture (replicating Experiment 1). The procedure of the experiment was identical to that used in Experiment 1. Again a fixed IPD was used for all participants to replicate the procedure of Experiment 1.

Results and discussion

A psychometric function was fit to each participant's responses for each of the sixteen stimulus types (2 Directions of Slant × 2 Viewing Distances × 4 Slants) to calculate the PSEs. The aspect ratios at the mean PSEs are shown in Figure 7. Figure 7A shows the aspect ratio data of the no-texture-scaling group. To examine the (slant) range effect, aspect ratio data from Experiment 1 in a similar range (9° to 27°) were also shown as colored lines. At a glance, there seems no prominent difference between the data of Experiment 1 and the data from the no-texture-scaling group. Because there is only one common slant (i.e., the 18°) between the two experiments, a two-sample t test was used to test whether the aspect ratio at the 18° slant differed between the two experiments for each of the four (Direction of Slant × Viewing Distance) combinations. The t test showed no difference for the pitch slant at 2 m, $t(36) = 0.39$, $p = 0.70$; no difference for the pitch slant at 8 m, $t(36) = 0.29$, $p = 0.77$; no difference for the yaw slant at 2 m, $t(37) = 1.44$, $p = 0.16$; and no difference for the yaw slant at 8 m, $t(36) = 0.19$, $p = 0.85$. This result supports the conclusion that there was no range effect. Figure 7B shows the aspect ratio data of the texture-scaling group. Compared to the aspect ratio data of the no-texture-scaling group, the aspect ratio data of the scaling group show a consistent elevation. A mixed effects regression of the complete data set found a main effect of texture scaling, $t(441) = 2.13$, $p = 0.034$. To compare the aspect ratio data from the texture-scaling group to that of Li and Durgin (2010), the aspect ratio data of Li and Durgin are also plotted (Figure 7B, colored lines). The data from the two studies are quite similar. Note that this suggests that the use of a fixed IPD in the present paper did not alter the results substantially.

A mixed effects regression of the complete data set found that aspect ratios were higher at farther than at nearer distance, $t(441) = 10.97$, $p < 0.0001$. Moreover,

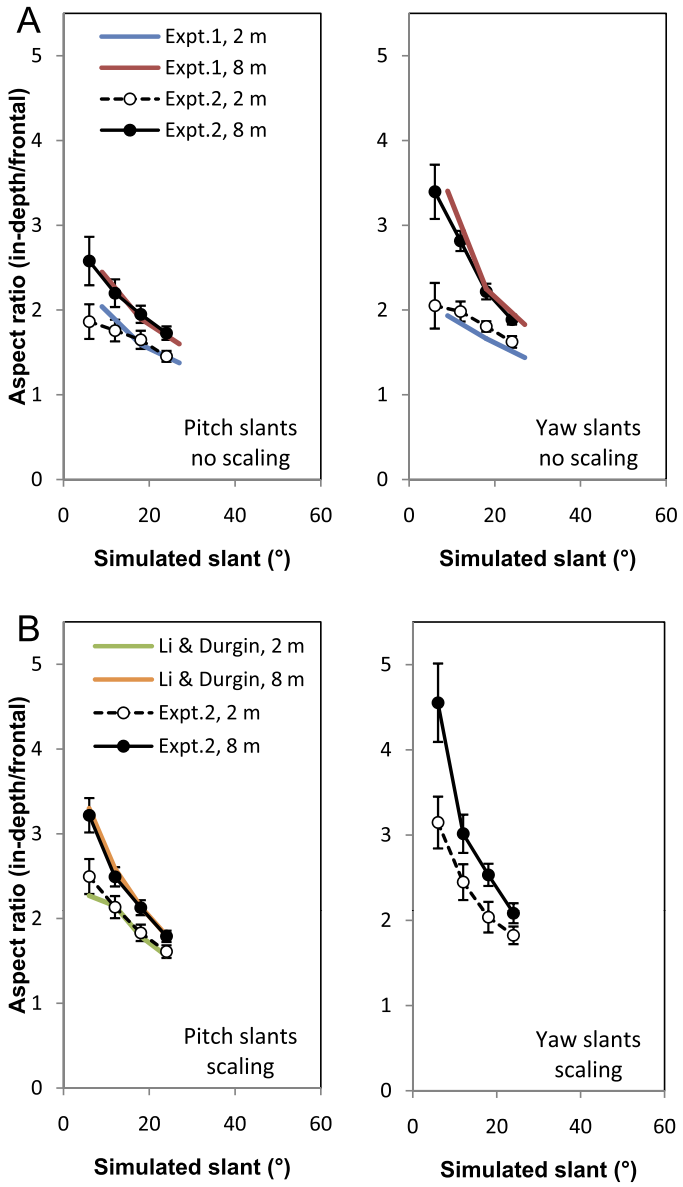

Figure 7. Results of Experiment 2. Aspect ratios at the mean PSEs for each of the Direction of Slant × Viewing Distance × Amount of Slant Combinations. Panel (A) shows the results of the group in which retinal texture size varied appropriately with viewing distance. Panel (B) shows the results of the texture scaling group for which texture scaling kept retinal texture size constant.

aspect ratios were higher for pitch slant than for yaw slant, $t(441) = 8.09$, $p < 0.0001$, which replicates the results in Experiment 1 in the absence of HVI correction. Because there was no frontal slant in Experiment 2, we could not correct the HVI effect for individual participant's data in Experiment 2 as we did in Experiment 1.

The main goal of Experiment 2 was to determine the source of the discrepancy between the results of Experiment 1 and the results of Li and Durgin (2010). Here we have shown that both patterns of results can be replicated depending on the presence (Li & Durgin, 2010) or absence (Experiment 1) of compensatory texture scaling, but that other factors (such as range of slants used) did not matter. Artificially scaling texture (and thus creating a conflicting source of information about changes in simulated viewing distance) seems to increase the bias in perceived aspect ratio and the bias in perceived slant.

Experiment 3

Whereas the results in Experiment 1 showed that the affine model based on mis-scaling of binocular disparity provided an excellent fit to the observed aspect ratio data, results in Experiment 2 indicated that the simple mis-scaling of binocular disparity may not be the only source of angular expansion in perceived slant. That is, mis-scaling of binocular disparity may only account for part of the slant overestimation we observed. This would predict that when using the affine model alone to fit the aspect ratio data, the required depth compression ratio, c, would be smaller than its true value (i.e., the affine model alone would require stronger depth compression than was actually present). To test whether this is the case, in Experiment 3, we sought to directly measure the depth compression ratio in our virtual environment. One technique to assess perceived viewing distance for stereoscopic scaling is the apparently circular cylinder (ACC) task (Johnston, 1991). Glennerster, Rogers, and Bradshaw (1996) pointed out some problems with this task (including the self-occlusion of the edges of a convex cylinder), and suggested using an apparent right dihedral angle task. So as to deal with some of the shortcomings of the ACC task without using a slope task, we instead implemented a version of the ACC task with a concave hemicylinder so that the entire surface would be visible. We also developed a simple ditch version of the experiment in which participants had to compare the height and depth of a horizontal cyclopean ditch specified by binocular disparity between the near and far surfaces.

Methods

Participants

Twenty Swarthmore undergraduates participated in Experiment 3. All had normal or corrected-to-normal vision. None of them had participated in Experiment 1 or 2. The experimental procedures reported here were approved by the local research ethics committee and

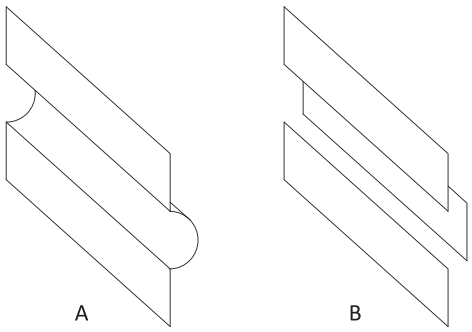

Figure 8. Diagrams of the stereoscopic stimuli (composed of random dots) used in Experiment 3. (A) Stimuli for the apparent hemi-cylinder task. (B) Stimuli for the ditch task.

were conducted in accordance with the Declaration of Helsinki.

Tasks

Participants wore the same nVisor HMD as used in Experiment 1 and performed three tasks successively—a figure discrimination task, an apparent hemicylinder task, and a ditch task. The figure discrimination task was always the first task. The order of the other two tasks was counterbalanced across participants. In the figure discrimination task, a random-dot stereogram was shown to the participant in each trial. The depicted stereo figure was a rectangle with rounded ends on one side and square ends on the other. The participant's task was to determine which side (left or right) had rounded ends. The main purpose of this task was to familiarize the participants with perceiving random-dot stereograms viewed through the HMD. In the apparent hemicylinder task, a random-dot stereogram depicting a concaved hemicylinder-like surface was shown in each trial (Figure 8A). The task was to judge whether the depth of the concave surface was deeper or shallower than that of a circular hemicylinder (i.e., half the vertical diameter). In the ditch task, the stereo figure was a single period square wave in depth, which looked like a ditch to the participants (Figure 8B). Participants had to determine whether the depth of the ditch was greater or less than the height (i.e., the vertical distance between the edges of the two near planes) of the ditch.

Stimuli and procedure

The IPD for each individual participant was measured before the experiment. The IPD value was then entered into the program to generate the random-dot stereogram stimuli for each participant. In the figure discrimination task, the simulated viewing distance to the stereo figure was 2 m. The vertical height of the figure subtended a visual angle of 12°. The simulated depth of the stereo figure was between 4.2 and 0.2 times the height. There were 36 trials in the discrimination task. In the apparent hemicylinder task, the simulated viewing distance to the flat part of the stereo figure was fixed. Two viewing distances (2 and 8 m) were tested in two successive sessions with the order being counterbalanced across participants. The vertical height of the hemicylinder-like surface subtended a fixed visual angle of 12°. The simulated depth of the hemicylinder-like surface varied from trial to trial. A logarithmic up-down staircase procedure was used to measure the point of subjective equality (PSE) between the depth and half-height. There were two interleaved staircases. One staircase started with a small depth to half-height ratio (1.1^{-10}) and the other started with a big depth to half-height ratio (1.1^{9}). Each staircase was sampled in random order in each of 15 mini blocks of two trials per block (30 trials total). On each trial, a two-alternative forced-choice (2AFC) response was collected by means of key presses (on a radio mouse) to indicate whether the depth extent appeared longer or shorter than the half height. The simulated depth to half-height ratio of the next trial in that staircase was adjusted up or down by a variable multiplicative step size (achieved by adding or subtracting from the exponent), depending on the response given and the block number in that staircase. Initial step size was by increasing or decreasing the exponent by eight; this step size declined to four after the first block and to two after the sixth block, where it remained thereafter. In the ditch task, the simulated viewing distance to the near plane of the ditch was fixed at 2 or 8 m. The vertical height of the ditch subtended a fixed visual angle of 12°. The depth of the ditch also varied from trial to trial. A similar logarithmic up-down staircase procedure as that used in the hemicylinder task was used, with the only exception that the PSE between the depth and whole-height of the ditch was measured. No feedback of the participants' performance was given in any of the three tasks.

Results and discussion

PSEs and 75% just noticeable differences (JNDs) were computed for the two tasks at each of the two distances for each participant using a logistic psychometric function on log aspect ratio. The mean PSEs and JNDs of the raw data of all the participants are shown in Table 1. A prominent feature of the results is that the Weber fraction (JND/PSE) for the ditch task is about twice that of the hemicylinder task, suggesting that shape judgments afforded more information than did pure stereoscopic depth judgments. Moreover, the PSEs and JNDs for the ditch task at the 8 m distance

Task	Distance	PSE	JND	WF
Hemicylinder	2 m	1.18	0.11	9.3%
Hemicylinder	8 m	2.62	0.24	9.2%
Ditch	2 m	1.34	0.23	17%
Ditch	8 m	6.73	1.16	17%

Table 1. Results of Experiment 3. The mean PSEs and mean JNDs and Weber fractions of the perceived depth/height (or half height) ratio in the hemicylinder task and in the ditch task.

are substantially larger than the mean PSEs and JNDs of the other three conditions. A post-experiment survey revealed that 17 out the 20 participants thought the ditch task was harder than the hemicylinder task. Several participants commented that they could not really tell the exact depth in the ditch task.

The results for both tasks suggested that the depth compression ratio in our virtual environment was about 0.75 to 0.85 (i.e., 1/1.34 to 1/1.18) at 2 m. Comparing these values to the affine model parameters in Figure 5 for the 2 m distance (i.e., 0.47) indicates that the directly measured depth compression ratios are insufficient to account for the misperception of slant in Experiment 1. This observation is consistent with our argument that affine compression based on mis-scaling of binocular disparity may only account for part of slant overestimation.

The difference between the ditch task and the hemicylinder task at 8 m shows that although there is clearly greater compression at the 8 m distance, the stereoscopic information at this distance is probably fairly limited in our apparatus (this may be partly due to image distortions remaining after software corrections for pincushion distortions in the optics of the lens system). In this case, the divergent estimates from the two different tasks emphasize that the mis-scaling of stereoscopic information may provide only a limited account of perceived slant. There have been prior reports that cylindrical shapes are more constantly perceived than rectangular shapes from stereopsis (Champion, Simmons, & Mamassian, 2004). However, the present difference between the ditch and ACC tasks could also be due to a differential density cues in the two tasks. Our algorithm for dot placement in the ACC task maintained orthographically projected density, but was viewed with perspective projection, and so there remained a subtle density gradient proportional to the simulated viewing distance to the dots. Density did not otherwise represent surface orientation, however. In the ditch task we had removed this cue by scaling the density of the farther surface so that retinal density was maintained.

Note that for the aspect ratio task in Experiment 1, the surfaces along which the balls were simulated were fully textured and were quite extended in depth, so the participants could typically use the richer information available in stereopsis from the entire hill surface (e.g., from surface texture information and from greater front-to-back depth) as well as orientation information from texture itself. The fact that the depth compression measured directly at the 2-m distance is insufficient to account for the compression observed in the slant task at the 2-m viewing distance implies either that compression was magnified when information was richer (which seems unlikely) or that the mis-scaling of stereoscopic information is an insufficient account of the misperception of surface orientation implied by the aspect ratio data of Experiment 1.

General discussion

In the present study, we measured the perceived aspect ratio of L-shaped arrangements of balls on tilted surfaces (9° to 90° with respect to the line of gaze) at two viewing distances and with four slant directions (uphill, downhill, leftward tilted, and rightward tilted). The results show that the perceived aspect ratio is systematically biased. The bias increases with viewing distance and the effect of viewing distance is more prominent with shallow slants, which replicates the findings of Li and Durgin (2010). There appears no prominent difference in the perceived aspect ratio between uphill and downhill slants and between leftward-tilted and rightward-tilted slants. Although the aspect ratio bias is consistently greater for yaw slants than that for pitch slants, this difference can be explained by the horizontal-vertical illusion. We also measured the perceived aspect ratio on tilted surfaces while manipulating the scale of the monocular size of the surface texture. It appears that the aspect ratio bias is smaller when the texture size is scaled appropriately to the viewing distance (and thus can serve as a relative-size cue to viewing distance) than when the texture size is held invariant with viewing distance.

The aspect ratio data obtained in Experiment 1 was used to evaluate the quality of three mathematical models that might explain the bias in perceived slant/aspect-ratio: i.e., the new optical slant model, the affine model based on mis-scaling of binocular disparity, and the intrinsic bias model. All three models provided reasonably good fits to the averaged aspect ratio data, though the model fits to individual subject's data revealed that fits from the new optical slant model and from the affine model were significantly better than that from the intrinsic bias model. A significant reason to doubt that the biases we have observed in perceived aspect ratio were due to the intrinsic bias of the perceived ground is that there was no difference in the aspect ratio data between pitch and yaw slant after the

HVI effect was taken into account, nor between uphill and downhill slants in pitch.

Whereas the results in Experiment 1 support the hypothesis that the mis-scaling of binocular disparity contributes to angular scale expansion in perceived optical slant, it seems likely that it is not the only source because the results in Experiment 3 showed that the depth compression ratios required by the affine model to best fit the aspect ratio data in Experiment 1 were smaller than the directly measured depth compression ratios at the near distance we used. This means the measured depth compression is not sufficient to account for the slant biases reflected in the aspect ratio data. Similar biases are found for slant estimates of real surfaces in near space where stereo information is thought to be well-calibrated (Durgin et al., 2010). There must, therefore, be other mechanisms that produce biases in perceived slant. However, reduced binocular scaling at far distances (Allison, Gillam, & Vecellio, 2009; Palmisano, Gillam, Govan, Allison, & Harris, 2010) suggests that effects of viewing distance on perceived slant may be mediated by binocular cues (Li & Durgin, 2010).

Because both the new optical slant model and the affine model based on mis-scaling of binocular disparity provided excellent fits to the aspect ratio data in Experiment 1, readers may wonder which model is better in modeling perceived optical slant in general. Whereas the affine model has a reasonable underlying mechanism (i.e., mis-scaling of binocular disparity), the new optical slant model provides a better fit to the explicit slant estimation data within reachable distance (Figure 2). One pronounced difference between the expected slant function based on the two models is that the slant function based on the affine model has a bias function that is roughly symmetrical around 45° of actual slant, whereas the slant function of the new optical slant model has a bias function with the peak bias skewed to the right of 45° of actual slant (around 50° to 60° from horizontal). Durgin et al. (2010) have observed that the verbal estimation of slanted surfaces within reach possess an error function with peak error skewed to about 60° (this bias was a spatial bias that peaked at about 60° from horizontal whether numeric estimates were made relative to vertical as 0°, or relative to horizontal as 0°, and thus were not verbal biases). It thus seems that to model explicit slant estimation data, the new optical slant model may be more appropriate. But to model the aspect ratio data, both models are good candidates, even though the amount of depth compression required by the affine model seems larger than that observed with stereograms in our HMD at a simulated viewing distance of 2 m.

A further advantage of the new optical slant model is that, like the optical slant model of Li and Durgin (2010), it takes distance into account and thus can be used to fit data across different viewing distances with a single parameter value. In contrast, the affine model based on the mis-scaling of stereoscopic depth does not yet include a means of taking distance into account and thus is free to adopt a different parameter value at each viewing distance (indeed it must). To better test the affine model, it would need to include a function representing the relationship between actual viewing distance and perceived viewing distance. Wagner's (1985) affine contraction and vector contraction (affine along the line of sight) models are based on larger viewing distances, but both assume a constant compression factor.

It is important to note that the affine depth compression model based on mis-scaling of binocular disparity is a powerful model only for explaining biases in space perception that are relevant to perceived optical slant (i.e., along the line of sight). Its power is very limited beyond that scope. For example, it cannot account for the overestimation in perceived downhill slope, when viewed from the top of a hill (Li & Durgin, 2009; Proffitt et al., 1995), which is a well-documented phenomenon of perceived geographical slant. It could account for the nonlinearly (i.e., increasingly) compressed exocentric distance (e.g., Gilinsky, 1951) by assuming the depth compression ratio decreases with viewing distance. But the same assumption could not explain distance estimation data and bisection data (e.g., Purdy & Gibson, 1955) suggesting that perceived egocentric distance is linearly compressed (i.e., with a constant compression ratio at different viewing distances) (see Loomis & Philbeck, 2008, for a recent review). In contrast, the angular expansion theory of slant has a companion model of perceived gaze direction or angular declination (which is not discussed in the present paper) to deal with all those phenomena quantitatively (Li & Durgin, 2012).

In general, even mechanistic models like stereoscopic mis-scaling must confront the problems of normalization, constancy, and calibration. If slant is systematically misperceived even in near space, why should this be? As Tyler (1980) has pointed out in his discussion of the tilted empirical horopter, our perceptual experience typically seems to be calibrated or normalized such that the vagaries of visual coding are opaque to us without special probing. The tilt of the empirical horopter does not generally make us misperceive vertical surfaces as tilted forward. So why are the orientations in between vertical and horizontal so systematically biased in perception? Why should slant perception be so different in this regard? Whereas mechanistic models propose that slant errors are incidental effects of perceptual error, the angular expansion hypothesis proposes that these may instead be functional coding choices (Durgin & Li, 2011; see also Durgin, 2009). Similar ideas have been cast in terms of Bayesian models of the likely

distribution of surface orientations (e.g., Girshick, Landy, & Simoncelli, 2011; Howe & Purves, 2005), and it may be that these kinds of strategic-coding formalizations provide a more fundamental form of explanation for why slant misperception can be understood in terms of angular scale expansion.

In conclusion, the present studies have extended the angular scale expansion theory (Durgin & Li, 2011) in three ways. First, we provided a unified optical slant model (i.e., Equation 3) that not only describes explicit slant estimation (0° to 90°) within reachable distance but can also account for implicit slant estimates (perceived aspect ratios) on slanted surfaces (9° to 90°) at the farther distances measured here. Second, once HVI effects are taken into account, the model can be applied to slant in yaw as well as in pitch. Third, the present results also suggest that affine depth compression based on mis-scaling of binocular disparity is a plausible mechanism for contributing to angular expansion in perceived optical slant (slant with respect to the line of sight). However, the contribution of depth compression may arise primarily in the effect of viewing distance. The angular scale expansion theory cannot be simply replaced by the affine model because the magnitude of depth compression actually observed in Experiment 3 seems inappropriate to account for observed slant biases in Experiment 1, but also because the angular expansion theory can account for a much wider range of spatial biases in space perception including the misperception of haptic slant in congenitally blind observers (e.g., Hajnal, Abdul-Malak, & Durgin, 2011), as well as the misperception of ground distance and of vertical height based on angular expansion of perceived gaze/angular declination. Thus the criterion of parsimony actually favors angular expansion theory rather than a piecemeal mechanistic account based entirely on the mis-scaling of disparity or the failure to properly encode that the ground plane is flat.

Keywords: slant, non-Euclidean, space perception, orientation, surface layout

Acknowledgments

This research was supported by Award Number R15 EY021026 from the National Eye Institute. The content is solely the responsibility of the authors and does not necessarily represent the official views of the National Eye Institute or the National Institutes of Health.

Commercial relationships: none.
Corresponding author: Frank H. Durgin.
Email: fdurgin1@swarthmore.edu.
Address: Psychology Department, Swarthmore College, Swarthmore, PA, USA.

References

Allison, R. S., Gillam, B. J., & Vecellio, E. (2009). Binocular depth discrimination and estimation beyond interaction space. *Journal of Vision, 9*(1):10, 1–14, http://www.journalofvision.org/content/9/1/10, doi:10.1167/9.1.10. [PubMed] [Article]

Battro, A. M., Netto, S. D. P., & Rozestraten, R. J. (1976). Riemannian geometries of variable curvature in visual space: Visual alleys, horopters, and triangles in big open fields. *Perception*, *5*(1), 9–23.

Bian, Z., & Andersen, G. J. (2011). Environmental surfaces and the compression of perceived visual space. *Journal of Vision*, *11*(7):4, 1–14, http://www.journalofvision.org/content/11/7/4, doi:10.1167/11.7.4. [PubMed] [Article]

Blank, A. A. (1953). The Luneburg theory of binocular visual space. *Journal of the Optical Society of America*, *43*(9), 717–721.

Bridgeman, B., & Hoover, M. (2008). Processing spatial layout by perception and sensorimotor interaction. *The Quarterly Journal of Experimental Psychology*, *61*(6), 851–859.

Champion, R. A., Simmons, D. R., & Mamassian, P. (2004). The influence of object size and surface shape on shape constancy from stereo. *Perception, 33,* 237–247.

Doumen, M. J., Kappers, A. M., & Koenderink, J. J. (2005). Visual space under free viewing conditions. *Perception & Psychophysics, 67*(7), 1177–1189.

Durgin, F. H. (2009). When walking makes perception better. *Current Directions in Psychological Science*, *18*(1), 43–47.

Durgin, F. H., & Li, Z. (2010). Controlled interaction: Strategies for using virtual reality to study perception. *Behavior Research Methods, 42*(2), 414–420.

Durgin, F. H., & Li, Z. (2011). Perceptual scale expansion: An efficient angular coding strategy for locomotor space. *Attention, Perception, & Psychophysics, 73*(6), 1856–1870.

Durgin, F. H., & Li, Z. (2012). Spatial biases and the haptic experience of surface orientation. In A. E. Saddik (Ed.), *Haptics, Rendering and Applications*. Rijeka, Croatia: InTech. Retrieved from: www.intechopen.com/books/haptics-rendering-and-applications/spatial-biases-and-the-haptic-experience-of-surface-orientation.

Durgin, F. H., Li, Z., & Hajnal, A. (2010). Slant perception in near space is categorically biased: Evidence for a vertical tendency. *Attention, Perception, & Psychophysics*, *72*(7), 1875–1889.

Foley, J. M. (1964). Desarguesian property in visual space. *Journal of Optical Society of America*, *54*(5), 684–690.

Foley, J. M. (1985). Binocular distance perception: egocentric distance tasks. *Journal of Experimental Psychology: Human Perception and Performance*, *11*(2), 133–149.

Foley, J. M., Ribeiro-Filho, N. P., & Da Silva, J. A. (2004). Visual perception of extent and the geometry of visual space. *Vision Research, 44*(2), 147–156.

Gilinsky, A. S. (1951). Perceived size and distance in visual space. *Psychological Review*, *58*(6), 460–482.

Girshick, A. R., Landy, M. S., & Simoncelli, E. P. (2011). Cardinal rules: Visual orientation perception reflects knowledge of environmental statistics. *Nature Neuroscience, 14*(7), 926–932.

Glennerster, A., Rogers, B. J., & Bradshaw, M. F. (1996). Stereoscopic depth constancy depends on the subject's task. *Vision Research, 36*(21), 3441–3456.

Hajnal, A., Abdul-Malak, D. T., & Durgin, F. H. (2011). The perceptual experience of slope by foot and by finger. *Journal of Experimental Psychology*: *Human Perception and Performance*, *37*(3), 709.

Hibbard, P. B., Goutcher, R., O'Kane, L. M., & Scarfe, P. (2012). Misperception of aspect ratio in binocularly viewed surfaces. *Vision Research*, *70*(1), 34–43.

Higashiyama, A. (1996). Horizontal and vertical distance perception: The discorded-orientation theory. *Perception & Psychophysics*, *58*(2), 259–270.

Howe, C. Q., & Purves, D. (2005). Natural-scene geometry predicts the perception of angles and line orientation. *Proceedings of the National Academy of Sciences, USA, 102*(4), 1228–1233.

Indow, T. (1991). A critical review of Luneburg's model with regard to global structure of visual space. *Psychological Review, 98,* 430–453.

Johnston, E. B. (1991). Systematic distortions of shape from stereopsis. *Vision Research*, *31*(7), 1351–1360.

Kammann, R. (1967). The overestimation of vertical distance and slope and its role in the moon illusion. *Perception & Psychophysics*, *2*(12), 585–589.

Kelly, J. W., Loomis, J. M., & Beall, A. C. (2004). Judgments of exocentric direction in large-scale space. *Perception, 33,* 443–454.

Koenderink, J. J., vanDoorn, A. J., & Lappin, J. S. (2000). Direct measurement of the curvature of visual space. *Perception, 29,* 69–79. doi:10.1068/p2921

Kudoh, N. (2005). Dissociation between visual perception of allocentric distance and visually directed walking of its extent. *Perception*, *34*(11), 1399.

Levin, C. A., & Haber, R. N. (1993). Visual angle as a determinant of perceived interobject distance. *Attention, Perception, & Psychophysics*, *54*(2), 250–259.

Li, Z., & Durgin, F. H. (2009). Downhill slopes look shallower from the edge. *Journal of Vision*, *9*(11):6, 1–15, http://www.journalofvision.org/content/9/11/6, doi:10.1167/9.11.6. [PubMed] [Article]

Li, Z., & Durgin, F. H. (2010). Perceived slant of binocularly viewed large-scale surfaces: A common model from explicit and implicit measures. *Journal of Vision*, *10*(14):13, 1–16, http://www.journalofvision.org/content/10/14/13, doi:10.1167/10.14.13. [PubMed] [Article]

Li, Z., & Durgin, F. H. (2012). A comparison of two theories of perceived distance on the ground plane: The angular expansion hypothesis and the intrinsic bias hypothesis. *i-Perception*, *3*(5), 368.

Li, Z., Phillips, J., & Durgin, F. H. (2011). The underestimation of egocentric distance: Evidence from frontal matching tasks. *Attention, Perception, & Psychophysics*, *73*(7), 2205–2217.

Li, Z., Sun, E., Strawser, C. J., Spiegel, A., Klein, B., & Durgin, F. H. (2013). On the anisotropy of perceived ground extents and the interpretation of walked distance as a measure of perception. *Journal of Experimental Psychology: Human Perception and Performance*, *39*(2), 477.

Loomis, J. M., Da Silva, J. A., Fujita, N., & Fukusima, S. S. (1992). Visual space perception and visually directed action. *Journal of Experimental Psychology: Human Perception and Performance*, *18*(4), 906–921.

Loomis, J. M., & Philbeck, J. W. (1999). Is the anisotropy of perceived 3-D shape invariant across scale?. *Attention, Perception, & Psychophysics*, *61*(3), 397–402.

Loomis, J. M., & Philbeck, J. W. (2008). *Measuring spatial perception with spatial updating and action*. New York, NY: Taylor & Francis.

Luneburg, R. K. (1947). *Mathematical analysis of binocular vision*. Princeton, NJ: Princeton University Press.

Luneburg, R. K. (1950). The metric of binocular visual space. *Journal of the Optical Society of America*, *40*(10), 627–640.

Norman, J. F., Crabtree, C. E., Clayton, A. M., & Norman, H. F. (2005). The perception of distances and spatial relationships in natural outdoor environments. *Perception*, *34*(11), 1315.

Ooi, T. L., & He, Z. J. (2007). A distance judgment function based on space perception mechanisms: Revisiting Gilinsky's (1951) equation. *Psychological Review, 114*(2), 441–454.

Ooi, T. L., Wu, B., & He, Z. J. (2006). Perceptual space in the dark affected by the intrinsic bias of the visual system. *Perception*, *35*(5), 605–624.

Palmisano, S., Gillam, B., Govan, D. G., Allison, R. S., & Harris, J. M. (2010). Stereoscopic perception of real depths at large distances. *Journal of Vision*, *10*(6):19, 1–16, http://www.journalofvision.org/content/10/6/19, doi:10.1167/10.6.19. [PubMed] [Article]

Philbeck, J. W., & Loomis, J. M. (1997). Comparison of two indicators of perceived egocentric distance under full-cue and reduced-cue conditions. *Journal of Experimental Psychology: Human Perception and Performance*, *23*(1), 72.

Proffitt, D. R., Bhalla, M., Gossweiler, R., & Midgett, J. (1995). Perceiving geographical slant. *Psychonomic Bulletin & Review*, *2*(4), 409–428.

Purdy, J., & Gibson, E. J. (1955). Distance judgment by the method of fractionation. *Journal of Experimental Psychology*, *50*(6), 374.

Ross, H. E. (1974). *Behaviour and perception in strange environments*. New York: Allen and Unwin.

Todd, J. T., Oomes, A. H., Koenderink, J. J., & Kappers, A. M. (2001). On the affine structure of perceptual space. *Psychological Science*, *12*(3), 191–196.

Tyler, C. W. (1980). Binocular moiré fringes and the vertical horopter. *Perception*, *9*(4), 475–478.

Wagner, M. (1985). The metric of visual space. *Attention, Perception, & Psychophysics*, *38*(6), 483–495.

Wagner, M. (2006). *The geometries of visual space*. Mahwah, NJ: Lawrence Erlbaum.

Appendix A. Fitting the aspect ratio data with the three slant models

Li and Durgin (2010) have shown that an aspect ratio task such as employed in Experiment 1 can be treated as an implicit measure of perceived optical slant. By assuming that biases in perceived aspect ratio are primarily due to biases in perceived optical slant, Li and Durgin provided the following formula (i.e., Equation A1) to model the relationship between perceived aspect ratio and perceived optical slant.

$$R = R' \frac{\sin(\beta')}{\sin(\beta)}, \tag{A1}$$

where R is the actual aspect ratio, R' is the perceived aspect ratio, β is the actual optical slant, and β' is the perceived optical slant.

In the present study, the aspect ratios at the PSEs correspond to the actual aspect ratios that were perceived as a ratio of one. That is, $R' = 1$. Thus, to predict the aspect ratios at the PSEs, we only need to know the perceived slant β'. The three models (i.e., the new optical slant model, the affine model based on mis-scaling of binocular disparity, and the intrinsic bias model) each assumes a different perceived slant function. Replacing β' with the corresponding slant function in Equation A1 would give us the formula to predict the aspect ratio data for the corresponding model. Equation A2 and A3 represent the assumed slant function for the optical slant model and for the intrinsic bias model respectively. The slant function for the affine model based on mis-scaling of binocular disparity is more complicated and is deduced in next section.

$$\beta' = 90° \cdot \sin(\beta) + k \cdot \ln(D) \cdot \cos(\beta) \tag{A2}$$

$$\beta' = \beta + \eta. \tag{A3}$$

Slant function of the affine model based on mis-scaling of binocular disparity

Binocular disparity provides a means to recover the 3-D structure of the physical environment from the two dimensional retinal images. Here we derive the expected perceived 3-D structure of a slanted surface if the observer misperceives the viewing distance to the fixation point so that binocular disparity information gets mis-scaled.

As shown in Figure A1 (left panel), the thick blue line represents a physical surface with a slant α. The center of the observer's head is at the origin and the fixation point is F. P is any given point on the slant and also on the sagittal plane of the observer.

The disparity between point P and fixation point F can be expressed by $\theta_p - \theta_f$. Since the interpupillary distance (ipd) for each observer is fixed, θ_p and θ_f only depend on the viewing distance to the two points (i.e., D_p and D_0 in Figure A1, right panel). That is, the disparity, δ, between P and F can be expressed as a function of D_p, D_0, and ipd:

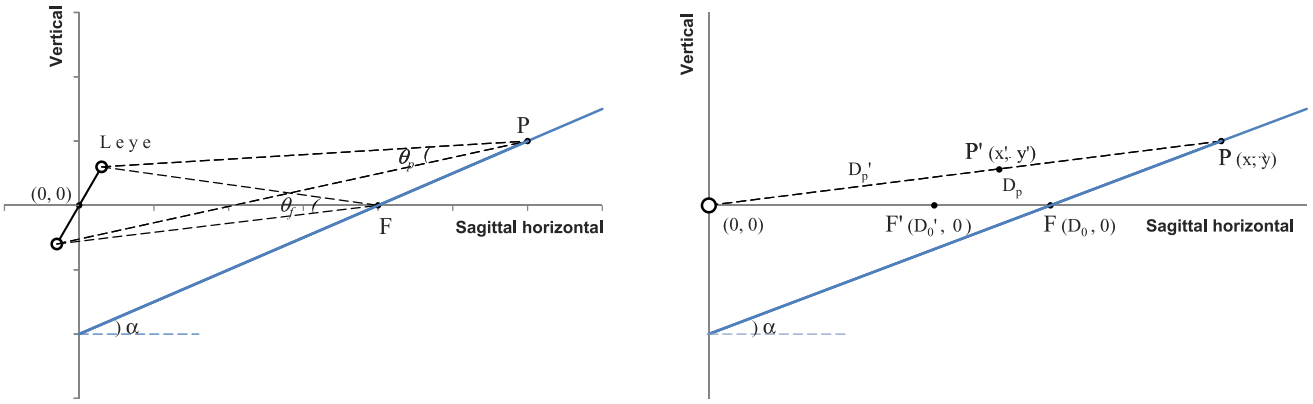

Figure A1. Geometric diagram used to illustrate the calculation of the perceived position of a given point *P* on a slant and also on the sagittal plane of the observer when the binocular disparity map is mis-scaled by the misperceived viewing distance to the fixation point *F*.

$$\delta = 2\tan^{-1}\left(\frac{ipd}{2D_p}\right) - 2\tan^{-1}\left(\frac{ipd}{2D_0}\right). \quad \text{(A4)}$$

As shown in Figure A1 right panel, let's assume that the viewing distance to the fixation point is foreshortened. That is, F is misperceived as F'. Similarly, the position of point P is also misperceived as P' (note, this is based on the assumption that the viewing direction to P is perceived accurately). Although the positions of P and F are both foreshortened, the relative disparity, δ, between them remained unchanged:

$$\delta = 2\tan^{-1}\left(\frac{ipd}{2D'_p}\right) - 2\tan^{-1}\left(\frac{ipd}{2D'_0}\right). \quad \text{(A5)}$$

Replacing δ in Equation A4 with Equation A5, and simplifying all the $\tan^{-1}(x)$ with x (because θ_p and θ_f should always be small), we obtain the formula to calculate the perceived viewing distance to point P:

$$D'_p = \frac{1}{D_p^{-1} + D_0'^{-1} - D_0^{-1}}. \quad \text{(A6)}$$

Because the origin, point P and point P' are collinear, the coordinate of P' (x', y') can be expressed by the coordinate of $P(x, y)$ with the following equations,

$$x' = \left(\frac{D'_p}{D_p}\right) \cdot x \quad \text{(A7)}$$

$$y' = \left(\frac{D'_p}{D_p}\right) \cdot y. \quad \text{(A8)}$$

Thus, if we know the perceived viewing distance to the fixation point F (equivalent to multiplying actual distance by the depth compression ratio), we can calculate the perceived position of any given point P on the slant and also on the sagittal plane of the observer using Equations A6, A7, and A8. That is how the affine model fits in Figure 2 and Figure 5 in the main text were obtained.

When calculating the perceived slant, we need to first calculate the perceived positions of several points along the surface of the slant and then obtain the slope of the linear fit of those perceived positions. We limit our analysis to a narrow field of view which is appropriate both because the human visual system can only handle disparities within a certain range (i.e., within the Panum's Area), and because in this range the mis-scaling is expected to approximate affine compression (apparent curvature may result from mis-scaling if a large field of view is considered). For the current analysis we limited our calculation to the points in a range that is 5° above and below the fixation point. In this range, the perceived surface of a flat slanted surface is still largely a flat surface but with a steeper slant.

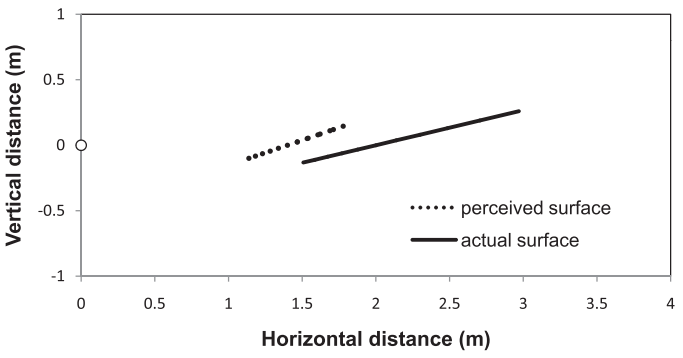

Figure A2. Predicted perceived slant (dotted line) of an actual 15° slant (solid line) at a viewing distance of 2 m based on the affine model assuming mis-scaling of binocular disparity. The observer is at the origin (the open circle) with a horizontal gaze, i.e., the fixation point on the actual surface is at point (2, 0). The depth compression ratio assumed in this example is 0.7.

Figure A2 shows the predictions of this analysis for a 15° surface (in this case positioned 2 m from the observer) under the assumption that the distance estimate used is only 70% of the true distance. The resulting perceived slant would be about 21°.

To illustrate how similar the predicted perceived slant based on the model of mis-scaling of binocular disparity is to that based on affine depth compression parallel to the line of sight, we computed the predicted perceived slant of surfaces from 6° to 90° at 2 m for depth compression ratios between 0.1 and 0.9. The results are plotted in Figure A3. It turns out that the prediction of the perceived slant based on the two models (i.e., lines vs. dots) is essentially identical. This verifies that a model based on the mis-scaling of binocular disparity (for a small field of view) is functionally equivalent to an affine model of depth compression parallel to the line of sight.

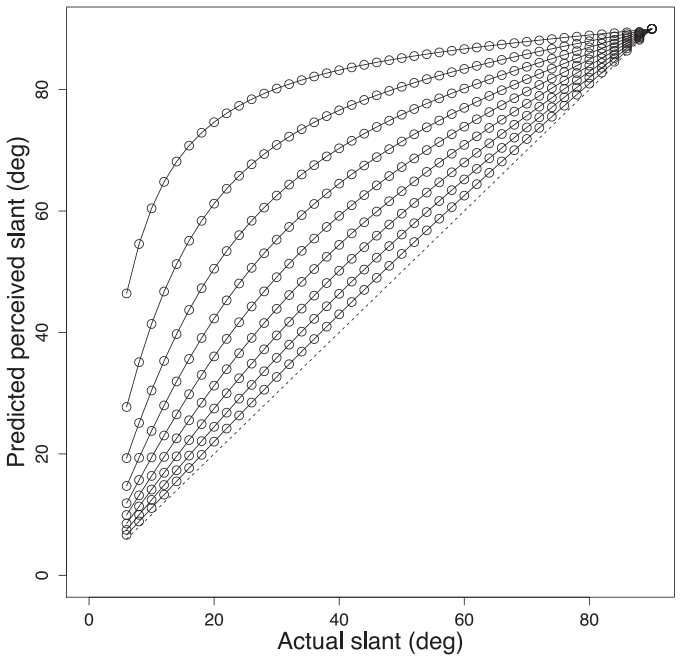

Figure A3. The predicted perceived slant functions based on the affine depth compression along line of sight (lines) and based on the mis-scaling of binocular disparity (open circles). The nine curves from top to bottom represent different assumed depth compression ratios from 0.1 to 0.9 (with intervals of 0.1). The simulated viewing distance was 2 m, but these functions are invariant with distance.